

UC Irvine

UC Irvine Previously Published Works

Title

WIMPlless dark matter in anomaly-mediated supersymmetry breaking with hidden QED

Permalink

<https://escholarship.org/uc/item/5846q2qk>

Journal

Physical Review D, 84(9)

ISSN

2470-0010

Authors

Feng, Jonathan L
Rentala, Vikram
Surujon, Ze'ev

Publication Date

2011-11-01

DOI

10.1103/physrevd.84.095033

Copyright Information

This work is made available under the terms of a Creative Commons Attribution License, available at <https://creativecommons.org/licenses/by/4.0/>

Peer reviewed

WIMPlless dark matter from an anomaly-mediated supersymmetry breaking hidden sector with no new mass parameters

Jonathan L. Feng,¹ Vikram Rantala,^{2,1} and Ze'ev Surujon¹¹*Department of Physics and Astronomy, University of California, Irvine, California 92697, USA*²*Department of Physics, University of Arizona, Tucson, Arizona 85721, USA*

(Received 28 November 2011; published 1 March 2012)

We present a model with dark matter in an anomaly-mediated supersymmetry breaking hidden sector with a $U(1) \times U(1)$ gauge symmetry. The symmetries of the model stabilize the dark matter and forbid the introduction of new mass parameters. As a result, the thermal relic density is completely determined by the gravitino mass and dimensionless couplings. Assuming nonhierarchical couplings, the thermal relic density is $\Omega_X \sim 0.1$, independent of the dark matter's mass and interaction strength, realizing the WIMPlless miracle. The model has several striking features. For particle physics, stability of the dark matter is completely consistent with R -parity violation in the visible sector, with implications for superpartner collider signatures; also the thermal relic's mass may be ~ 10 GeV or lighter, which is of interest given recent direct detection results. Interesting astrophysical signatures are dark matter self-interactions through a long-range force, and massless hidden photons and fermions that contribute to the number of relativistic degrees of freedom at big bang nucleosynthesis and cosmic microwave background. The latter are particularly interesting, given current indications for extra degrees of freedom and near future results from the Planck observatory.

DOI: 10.1103/PhysRevD.85.055003

PACS numbers: 95.35.+d, 12.60.Jv

I. INTRODUCTION

The astrophysical evidence for dark matter is overwhelming, but the mass and nongravitational interactions of dark matter are unknown. Under certain assumptions, however, one can place bounds on these parameters. One of the most interesting scales in high-energy physics is the weak scale $v = 246$ GeV, which is currently being probed by the Large Hadron Collider (LHC). The framework of weakly interacting massive particle (WIMP) dark matter ties the mass and interaction strength of a thermal relic dark matter particle to electroweak physics. WIMPs, which are defined as particles with weak-scale masses and couplings, naturally freeze-out with the right relic density, since

$$\Omega_X \propto \frac{1}{\langle \sigma_{\text{an}} v \rangle} \sim \frac{m_{\text{weak}}^2}{g_{\text{weak}}^4}, \quad (1)$$

and for $g_{\text{weak}} \sim 0.6$ and $m_{\text{weak}} \sim v$, the thermal relic density Ω_X is near the desired value $\Omega_{\text{DM}} \approx 0.23$. Since theories that explain the hierarchy problem almost always introduce new weak-scale particles, they also typically can include WIMP dark matter.

At the same time, Eq. (1) implies that even particles with different masses and couplings may have the right thermal relic density, provided they have the same ratio m/g^2 as WIMPs [1,2]. As an example, such WIMPlless dark matter may arise in hidden sectors of gauge-mediated supersymmetry (SUSY)-breaking models, provided that messengers generate similar SUSY-breaking mass scales in the visible and hidden sectors. The possibility of dark matter with the correct thermal relic density, but masses and couplings that

differ, possibly drastically, from WIMPs, opens up many new avenues for dark matter detection [1–14].

Recently it has been shown [15,16] that models with anomaly-mediated supersymmetry breaking (AMSB) [17,18] may also give rise to WIMPlless dark matter, without depending on messengers. In AMSB, superpartner masses scale as $m \sim (g^2/16\pi^2)M_{3/2}$, where $M_{3/2}$ is the gravitino mass, a universal relation that holds for all sectors, visible and hidden. Hidden sectors, if they exist, therefore generically have particles with the same ratio $m/g^2 \sim M_{3/2}/16\pi^2$ as WIMPs, and these particles are therefore natural WIMPlless candidates.

The visible sector in AMSB models enjoys the safety of being minimally flavor violating [19–22]. It is also highly predictive, as all the new physics parameters are determined by the standard model (SM) Yukawa and gauge couplings, along with three dimensionful parameters: $M_{3/2}$, μ , and B . For example, gaugino masses are fixed, relative to the gravitino mass, by the beta-functions to be

$$M_1:M_2:M_3:M_{3/2} \approx 3.3:1:-10:370. \quad (2)$$

Unfortunately, the AMSB framework also has problems: in its minimal realization, sleptons are tachyonic, and the usual lightest supersymmetric particle, the neutral Wino, has the right relic abundance only for $m_{\tilde{W}} \sim 3$ TeV, implying an unnaturally large gluino mass $m_{\tilde{g}} \sim 30$ TeV [18].

We will assume that the tachyonic slepton problem is solved, perhaps by one of the mechanisms in the literature; see, for example, Refs. [23–25]. As for the second problem, since 30 TeV gluinos would reintroduce the hierarchy problem, we may take it as a hint that the Wino is not a

major component of dark matter. The Wino dark matter problem may be traced back to the fact that SU(2) is nearly conformal in the minimal supersymmetric standard model (MSSM), and so the Wino is “accidentally” light for its couplings. In a hidden sector, however, there is much more freedom in choosing gauge symmetries and particle content. We will take advantage of this and show that WIMPlless dark matter can originate from a U(1) × U(1) hidden sector. Note that, in the models we present, the visible sector is relieved from its duty to provide dark matter, and the hidden dark matter particle is stabilized even without *R* parity. The possibility of AMSB with *R*-parity violation is interesting by itself [26] and does not require a hidden sector, as the dark matter may have another origin. However, this framework provides a concrete example in which dark matter with a naturally correct thermal relic density is perfectly consistent with broken *R* parity, with implications for SUSY searches at colliders and elsewhere.

As noted above, WIMPlless dark matter in AMSB has been explored in two previous studies [15,16]. Although these have only scratched the surface of all model-building possibilities, it is perhaps helpful to place this study in the context of the previous two. WIMPlless dark matter requires that there be a bath of light particles for the dark matter to annihilate to. A natural possibility is that this thermal bath is composed of massless gauge bosons.¹ It is, then, important that the gauge symmetry not be broken (at least until freeze-out). In AMSB, the generic expression for scalar soft masses is

$$m_0^2 \sim (y^4 - y^2 g^2 - b g^4) \left(\frac{M_{3/2}}{16\pi^2} \right)^2, \quad (3)$$

where *y* and *g* denote Yukawa and gauge couplings, respectively, *b* is the one-loop beta-function coefficient (with *b* < 0 for asymptotically free theories), and positive $\mathcal{O}(1)$ coefficients in front of each term have been suppressed. In Ref. [15], asymptotically-free hidden sectors without Yukawa couplings were considered. Since *b* < 0 for these sectors, $m_0^2 > 0$, and SUSY breaking did not break the gauge symmetry. Provided the confinement scale was sufficiently low, gauge bosons formed the thermal bath. In Ref. [16], we considered Abelian models without Yukawa couplings, where *b* > 0, but tachyonic scalars were avoided by invoking μ terms to raise the scalar masses. This led to some extremely simple scenarios. However, to realize the WIMPlless miracle in its purest form, these models required a mechanism to generate μ terms of the same order as the SUSY-breaking parameters, as discussed in Ref. [16].

In this paper we present another model with Abelian gauge symmetries, but with masses completely determined

¹Goldstone bosons and chiral fermions are other possibilities [15].

by AMSB-induced soft SUSY-breaking parameters. Tachyonic scalars are avoided by introducing Yukawa couplings, which raise the scalar masses and allow us to construct a stable minimum for the scalar potential without introducing a supersymmetric μ term by hand. The model has a U(1) × U(1) gauge symmetry and 6 chiral superfields. The existence of a second U(1) (which is ultimately spontaneously broken) and one more field compared to the models of Ref. [16] are needed to stabilize the potential without introducing supersymmetric μ terms by hand. The other chiral fields are required for anomaly cancellation. Some of the particles, together with the hidden photon, remain massless and contribute to the number of extra degrees of freedom probed by big bang nucleosynthesis (BBN) and the cosmic microwave background (CMB). Another prediction of the model is that the dark matter candidate has long-range self-interactions. Both the new massless degrees of freedom and the self-interactions can be probed by current and future astrophysical observations.

In the sections below, all particles and fields are in the hidden sector unless otherwise noted, and we use MSSM-like notation for the superfields and component fields. For example, \hat{e} , \tilde{e} , and *e* denote a hidden electron superfield, selectron, and electron, respectively, and \hat{H} , *H*, and \tilde{H} denote a hidden Higgs superfield, Higgs boson, and Higgsino.

II. MODEL-BUILDING CONSIDERATIONS

The simplest Abelian model, supersymmetric QED (SQED), has the generic problem of tachyonic sleptons in AMSB. For concreteness, consider SQED with one light flavor (\hat{e}_+ , \hat{e}_-). The positive beta-function implies that the soft selectron mass parameters are negative, breaking the U(1) spontaneously. By itself, this is not necessarily a problem, since the U(1) is hidden. However, the resulting quartic term in the potential,

$$V_D = \frac{g^2}{2} (|\tilde{e}_+|^2 - |\tilde{e}_-|^2)^2, \quad (4)$$

has a *D*-flat direction along

$$|\tilde{e}_+| = |\tilde{e}_-|, \quad (5)$$

rendering the model unstable.

There are a few ways to stabilize the potential. First, supergravity interactions would presumably stabilize the potential in any event. However, if this is the dominant stabilizing effect, the scalars would acquire vacuum expectation values (VEVs) at the Planck scale. Whether such an effect is parameterized by a hard SUSY-breaking quartic or by some higher-dimensional operator, it would be related to Planck-scale physics and therefore would not yield a viable WIMPlless dark matter candidate.

Another way to stabilize the potential is to introduce a supersymmetric μ term by hand [16]. The obvious drawback of this approach is that a new mass scale is being

introduced, thereby spoiling the natural WIMPLESS relation unless there is a mechanism that generates it at the right scale, $\mu \sim g^2 M_{3/2}/(16\pi^2)$. The tachyon problem in SQED is therefore transformed into a μ problem. Note, however, the difference between SQED and the MSSM: the former is a vectorlike theory and allows for μ terms for the sleptons. In contrast, the MSSM lepton sector is chiral, and requires extending the physical content of the theory to solve the tachyonic slepton problem.

Here we will take a different approach that uses Yukawa interactions in the hidden sector to stabilize the scalar potential. Recall the generic expression for scalar soft masses given in Eq. (3). The presence of Yukawa interactions lifts the scalar masses and may stabilize the potential. Of course, to allow Yukawa interactions, the field content must be extended.

Perhaps the simplest extension of the SQED model above is obtained by adding one gauge singlet superfield \hat{H} . We may impose a discrete Z_3 symmetry to avoid μ terms. The most generic renormalizable superpotential is then

$$W = y\hat{H}\hat{e}_+\hat{e}_- + \frac{1}{6}\kappa\hat{H}^3. \quad (6)$$

Note that a nonzero value for κ explicitly breaks the (anomalous) global Peccei-Quinn (PQ) symmetry under which \hat{H} has charge 2 and \hat{e}_+ and \hat{e}_- both have charge -1 . Including the new F terms, the resulting scalar potential is

$$V_{\text{SUSY}} = \frac{g^2}{2}(|\tilde{e}_+|^2 - |\tilde{e}_-|^2)^2 + |y|^2(|H|^2|\tilde{e}_+|^2 + |H|^2|\tilde{e}_-|^2) + \left| \frac{1}{2}\kappa H^2 + y\tilde{e}_+\tilde{e}_- \right|^2. \quad (7)$$

The D -flat directions are lifted when y and κ are nonzero. The soft SUSY-breaking parameters are

$$\begin{aligned} m_{\tilde{\gamma}} &= \frac{g^2}{8\pi^2} M_{3/2}, \\ m_{\tilde{e}_\pm}^2 &= \left[-1 - \left(\frac{y}{g}\right)^2 + \frac{3}{4}\left(\frac{y}{g}\right)^4 + \frac{1}{8}\left(\frac{y}{g}\right)^2\left(\frac{\kappa}{g}\right)^2 \right] m_{\tilde{\gamma}}^2, \\ m_H^2 &= \left[-\left(\frac{y}{g}\right)^2 + \frac{3}{4}\left(\frac{y}{g}\right)^4 + \frac{1}{2}\left(\frac{y}{g}\right)^2\left(\frac{\kappa}{g}\right)^2 + \frac{3}{16}\left(\frac{\kappa}{g}\right)^4 \right] m_{\tilde{\gamma}}^2, \\ A_{H\tilde{e}_+\tilde{e}_-} &= y \left[2 - \frac{3}{2}\left(\frac{y}{g}\right)^2 - \frac{1}{4}\left(\frac{\kappa}{g}\right)^2 \right] m_{\tilde{\gamma}}, \\ A_{HHH} &= -\frac{3}{4}\kappa \left[2\left(\frac{y}{g}\right)^2 + \left(\frac{\kappa}{g}\right)^2 \right] m_{\tilde{\gamma}}. \end{aligned} \quad (8)$$

Now that the D -flat directions are lifted, we examine this potential for (meta-)stable minima. For one of these vacua to have a WIMPLESS dark matter candidate, it must satisfy several additional criteria:

- (i) There should be at least one stable massive particle that plays the role of dark matter.

- (ii) There must be at least one light particle that serves as the thermal bath.
- (iii) The heavy dark matter particles must have tree-level annihilations to the particles in the thermal bath to naturally get the right relic density.

To examine the minima of the potential, we may begin by making various assumptions for which fields acquire VEVs. Given one such assumption, we then determine if there are ranges of the parameters y/g and κ/g that give rise to stable minima with suitable WIMPLESS candidates. The possible symmetries that can prevent a heavy particle from decaying into the thermal bath are electric charge, Lorentz symmetry (the lightest fermion is stable), R parity and, if $\kappa \rightarrow 0$, the global PQ symmetry. The particles that are potentially light and can make up the thermal bath are the photon, the electrons, the Higgsino, and, if $U(1)_{\text{PQ}}$ is a good symmetry and is spontaneously broken, there may also be a light Goldstone boson of the PQ symmetry. However, in certain vacua, some (or all) of these are massive. Here are a few sample cases:

- (i) None of the fields acquires a VEV: in this scenario, the photon, the electron, and the Higgsino, are all massless. However, none of the massive particles is stable, since the decays $H \rightarrow e_+e_-$, $\tilde{e}_\pm \rightarrow \tilde{H}\tilde{e}_\mp$, and $\tilde{\gamma} \rightarrow \tilde{H}e_+e_-$, are all allowed. There is therefore no cold dark matter candidate.
- (ii) H acquires a VEV, but \tilde{e}_+ and \tilde{e}_- do not. Note that this pattern of VEVs may be realized in some regions, although Eq. (8) implies $m_H^2 > m_{\tilde{e}_\pm}^2$. In this case, the gauge symmetry is unbroken, so the photon is still massless. The fermions all become massive, and the lightest one is stable. Unfortunately, the model is constrained enough that the lighter of the Higgsino and photino is always stable, since all its decay modes are kinematically forbidden. The Higgsino and photino do not have tree-level annihilations to photons, and so would typically overclose the Universe.
- (iii) \tilde{e}_+ , \tilde{e}_- and H acquire VEVs. These VEVs break the gauge symmetry. In general, the electrons and Higgsino will be massive in these vacua. The only potential candidate for the thermal bath is the pseudo-Goldstone boson of the PQ symmetry breaking (in the $\kappa \rightarrow 0$ limit). This scenario merits further study, but we note that the dark matter would annihilate through derivative couplings, and therefore would not realize the WIMPLESS miracle, at least in its purest form.

Although this simple Yukawa extension of SQED does not appear to provide us with a WIMPLESS dark matter candidate, it illustrates many of the potential problems and also suggests several ideas for model building. In the next section, we will present a model that provides a viable WIMPLESS dark matter candidate.

III. A U(1) × U(1) MODEL

Recall that Eq. (8) implies that the singlet extension of the SQED model above satisfies the relation $m_H^2 > m_{\tilde{e}_\pm}^2$ everywhere throughout its parameter space. Although this by itself did not forbid the existence of vacua with $\langle H \rangle \neq 0$ and $\langle \tilde{e}_\pm \rangle = 0$, the constrained nature of AMSB made it impossible to find a viable region without a neutralino overabundance. Therefore, we wish to modify the singlet-added SQED model above so that $m_H^2 < m_{\tilde{e}_\pm}^2$ can hold. One would hope that such a model would more easily realize $\langle H \rangle \neq 0$ and $\langle \tilde{e}_\pm \rangle = 0$ simultaneously.

To do this, we introduce a new U(1) gauge symmetry under which the singlet is charged. This gives rise to an additional negative contribution to m_H^2 . We choose to gauge the PQ symmetry, namely, the U(1) that is ‘‘axial’’ with respect to the electron. However, to make the theory anomaly-free, we must introduce additional chiral superfields.

Perhaps the simplest choice is a mirror duplicate sector with all the charges inverted. This model has a $U(1)_A \times U(1)_B$ gauge symmetry with gauge couplings g_A and g_B , respectively. We also impose a Z_3 symmetry to forbid μ terms. The field content and the charges are given in Table I. Dark matter is stabilized by hidden lepton flavor conservation. R parity (R_p) is conserved, but it will play no role in stabilizing dark matter. We will use it only to distinguish between ‘‘ordinary’’ and ‘‘superpartner’’ fields.

The most generic superpotential is

$$W = y_e \hat{H}_e \hat{e}_+ \hat{e}_- + y_\mu \hat{H}_\mu \hat{\mu}_+ \hat{\mu}_-. \quad (9)$$

The model has four supersymmetric dimensionless couplings: g_A , g_B , y_e , and y_μ . However, constraints from model building and from the dark matter relic density will depend only on the three ratios

$$\tilde{g}_B \equiv \frac{g_B}{g_A}, \quad \tilde{y}_e \equiv \frac{y_e}{g_A}, \quad \tilde{y}_\mu \equiv \frac{y_\mu}{g_A}. \quad (10)$$

Since annihilation of dark matter proceeds exclusively through A -photon interactions, and so the annihilation cross section is proportional to g_A^4 , it is useful to express all the masses in terms of $M_{\tilde{A}}$. The soft SUSY-breaking parameters induced by AMSB are, then,

TABLE I. Superfields and their charges in the U(1) × U(1) model.

| | \hat{e}_+ | \hat{e}_- | \hat{H}_e | $\hat{\mu}_+$ | $\hat{\mu}_-$ | \hat{H}_μ |
|----------|-------------|-------------|-------------|---------------|---------------|---------------|
| $U(1)_A$ | 1 | -1 | 0 | -1 | 1 | 0 |
| $U(1)_B$ | 1 | 1 | -2 | -1 | -1 | 2 |
| $U(1)_e$ | 1 | -1 | 0 | 0 | 0 | 0 |
| Z_3 | 1 | 1 | 1 | 1 | 1 | 1 |
| R_p | - | - | + | - | - | + |

$$\begin{aligned} M_{\tilde{A}} &= \frac{g_A^2}{4\pi^2} M_{3/2}, & M_{\tilde{B}} &= 3\tilde{g}_B^2 M_{\tilde{A}}, \\ m_{\tilde{e},\tilde{\mu}}^2 &= \left(-\frac{1}{2} - \frac{1}{4}\tilde{y}_{e,\mu}^2 + \frac{3}{16}\tilde{y}_{e,\mu}^4 - \frac{3}{4}\tilde{y}_{e,\mu}^2\tilde{g}_B^2 - \frac{3}{2}\tilde{g}_B^4 \right) M_{\tilde{A}}^2, \\ m_{H_{e,\mu}}^2 &= \left(-\frac{1}{4}\tilde{y}_{e,\mu}^2 + \frac{3}{16}\tilde{y}_{e,\mu}^4 - \frac{3}{4}\tilde{y}_{e,\mu}^2\tilde{g}_B^2 - 6\tilde{g}_B^4 \right) M_{\tilde{A}}^2, \\ A_{e,\mu} &= \tilde{y}_{e,\mu} \left(1 - \frac{3}{4}\tilde{y}_{e,\mu}^2 + 3\tilde{g}_B^2 \right) g_A M_{\tilde{A}}. \end{aligned} \quad (11)$$

We are interested in solutions where at least one of the Higgs fields acquires a VEV, but the selectrons and smuons do not. In this case, the A photon remains massless and provides the thermal bath. Note that the relevant quartic term,

$$V_{D_B} = \frac{1}{2} g_B^2 (-2|H_e|^2 + 2|H_\mu|^2)^2, \quad (12)$$

has a D -flat direction along $|H_e| = |H_\mu|$. To maintain stability of the potential, the mass parameter along this direction must therefore be positive, yielding the condition

$$m_{H_e}^2 + m_{H_\mu}^2 > 0. \quad (13)$$

It follows that only one of the Higgs bosons can acquire a VEV. Without loss of generality, we choose this field to be H_e . Minimizing the potential results in

$$\langle H_e \rangle^2 = \frac{-m_{H_e}^2}{4g_B^2}. \quad (14)$$

This VEV generates masses for the electrons and the B -gauge boson, and it contributes to the masses of the selectrons and neutralinos.

In the bosonic sector, the physical Higgs and the B -gauge boson both acquire the same mass,

$$m_{H_e^0}^2 = M_B^2 = -2m_{H_e}^2. \quad (15)$$

The selectron and smuon masses are

$$\begin{aligned} \Delta V &= \begin{pmatrix} \tilde{e}_+ & \tilde{e}_-^* \end{pmatrix} \begin{pmatrix} m_{\tilde{e}_+}^2 - 2g_B^2 \langle H_e \rangle^2 + |y_e|^2 \langle H_e \rangle^2 & A_e \langle H_e \rangle \\ A_e^* \langle H_e \rangle & m_{\tilde{e}_-}^2 - 2g_B^2 \langle H_e \rangle^2 + |y_e|^2 \langle H_e \rangle^2 \end{pmatrix} \begin{pmatrix} \tilde{e}_+^* \\ \tilde{e}_- \end{pmatrix} \\ &+ (m_{\tilde{\mu}_+}^2 + 2g_B^2 \langle H_e \rangle^2) |\tilde{\mu}_+|^2 + (m_{\tilde{\mu}_-}^2 + 2g_B^2 \langle H_e \rangle^2) |\tilde{\mu}_-|^2. \end{aligned} \quad (16)$$

The resulting mass eigenvalues of the selectrons are

$$\begin{aligned} m_{\tilde{e}_2}^2 &= m_{\tilde{e}}^2 - 2g_B^2 \langle H_e \rangle^2 + |y_e|^2 \langle H_e \rangle^2 + |A_e| \langle H_e \rangle, \\ m_{\tilde{e}_1}^2 &= m_{\tilde{e}}^2 - 2g_B^2 \langle H_e \rangle^2 + |y_e|^2 \langle H_e \rangle^2 - |A_e| \langle H_e \rangle. \end{aligned} \quad (17)$$

Note that we have used $m_{\tilde{e}}^2 = m_{\tilde{e}_+}^2 = m_{\tilde{e}_-}^2$. The singlet H_μ acquires a negative contribution to its mass from the D -term, such that its physical mass is

$$(m_{H_\mu}^{\text{phys}})^2 = m_{H_\mu}^2 - 4g_B^2 \langle H_e \rangle^2 = m_{H_e}^2 + m_{H_\mu}^2. \quad (18)$$

We see that requiring the D -flat direction to be stable, Eq. (13), is equivalent to requiring $(m_{H_\mu}^{\text{phys}})^2 > 0$, as expected.

In the fermionic sector, e_+ and e_- combine into one Dirac fermion, the electron e , with mass $m_e = y_e \langle H_e \rangle$. The muons are massless and form part of the thermal bath. There are four neutralinos in the model: \tilde{A} and two combinations of \tilde{B} and \tilde{H}_e are massive, but \tilde{H}_μ is massless and is part of the thermal bath.

The rough picture of the spectrum is therefore:

- (i) Massive particles: 1 B -gauge field, 1 physical Higgs (H_e), 1 Dirac electron (e), 3 heavy neutralinos ($\tilde{A}, \tilde{B}, \tilde{H}_e$), and 5 complex scalars ($H_\mu, \tilde{e}_{1,2}, \tilde{\mu}_\pm$).
- (ii) Massless particles: 1 A -photon, 1 Higgsino (\tilde{H}_μ), and 2 Weyl muons (μ_\pm).

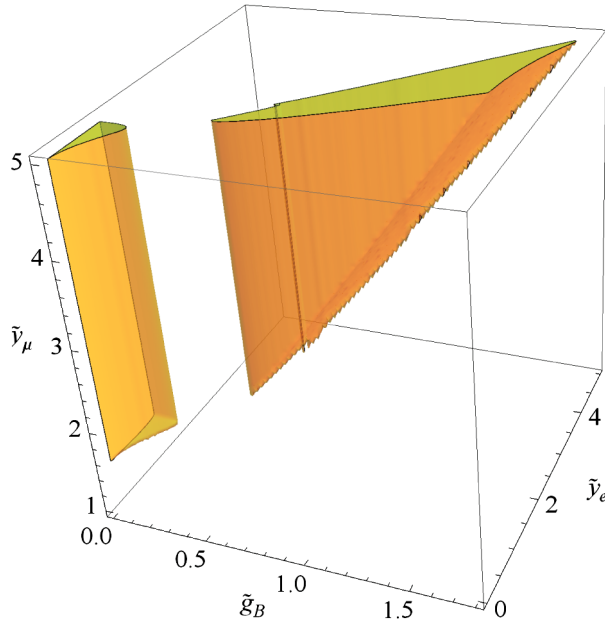


TABLE II. Various decay channels for the heavy fields. If $m_{\tilde{e}_1} > m_e$, the lighter selectron decays through $\tilde{e}_1 \rightarrow e\tilde{A}^{(*)}$, and if $m_e > m_{\tilde{e}_1}$, the electron decays through $e \rightarrow \tilde{e}_1\tilde{A}^{(*)}$, but the lighter of \tilde{e}_1 and e is stable and forms dark matter.

| Particle | Sample decay channel |
|---|-----------------------------|
| Heavy gauge boson B | $\mu_+ \mu_-$ |
| Electron-type Higgs H_e | AA |
| Neutralinos ($\tilde{A}, \tilde{B}, \tilde{H}_e$) | $\mu_+ \mu_- \tilde{H}_\mu$ |
| Muon-type Higgs H_μ | $AA, \mu_+ \mu_-$ |
| Smuons $\tilde{\mu}_\pm$ | $\mu_\pm \tilde{H}_\mu$ |
| Heavy selectron \tilde{e}_2 | $\tilde{e}_1 A$ |

The potential candidates for dark matter are either the electron or the lighter selectron \tilde{e}_1 , with the lighter of these being stabilized by an accidental global $U(1)$ symmetry analogous to lepton flavor. Note that the mass of the dark matter particle is independent of \tilde{y}_μ , as long as \tilde{y}_μ is in a viable region of parameter space, as can be seen in Fig. 1. (A weak dependence will appear once higher-order corrections are included). All the other massive particles decay to a combination of the dark matter particle and the massless fields. The various decay channels are listed in Table II.

Figure 1 shows the viable regions in the $(\tilde{g}_B, \tilde{y}_e, \tilde{y}_\mu)$ parameter space, namely, those regions where $U(1)_A$ is not broken (selectrons/smuons do not acquire a VEV, and

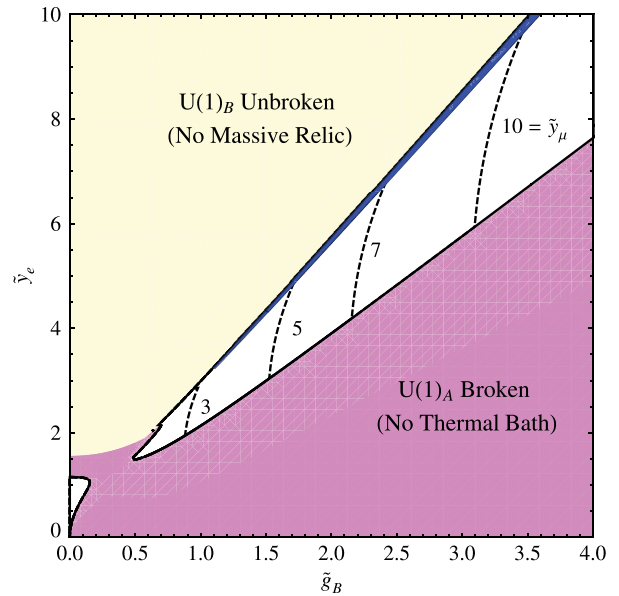


FIG. 1 (color online). *Left*: Allowed regions in the $(\tilde{g}_B, \tilde{y}_e, \tilde{y}_\mu)$ parameter space of the $U(1)_A \times U(1)_B$ model. *Right*: A projection of the allowed parameter space onto the $(\tilde{g}_B, \tilde{y}_e)$ plane. The light yellow and medium magenta shaded regions are excluded for the reasons indicated. Dark matter is composed of selectrons everywhere in the viable region, except inside the dark blue band, where it is electrons. At tree-level, the mass of the dark matter particle is independent of \tilde{y}_μ , as long as \tilde{y}_μ is in a viable region of parameter space. Contours of minimum \tilde{y}_μ for given values of $(\tilde{g}_B, \tilde{y}_e)$ are shown. Regions to the right of the $\tilde{y}_\mu = \text{const}$ curves are not viable for $\tilde{y}_\mu > \text{const}$, since the constraint $m_{H_e}^2 + m_{H_\mu}^2 > 0$ cannot hold, and the potential is unstable.

massless photons provide the thermal bath), $U(1)_B$ is broken (H_e acquires a VEV, providing mass for the electrons), and the potential along the D -flat direction is stabilized ($m_{H_e}^2 + m_{H_\mu}^2 > 0$). Although most of the viable region admits scalar dark matter (\tilde{e}_1), dark matter is made of fermions (e) in the narrow dark blue band. This region has a small Higgs VEV $\langle H_e \rangle$, and thus the electron is lighter than the selectrons. At another boundary of the scalar dark matter region the scalars become massless. Beyond that boundary, $U(1)_A$ is spontaneously broken and there is no viable WIMPlless dark matter.

IV. RELIC DENSITY

The thermal relic density of a dark matter particle X annihilating via S -wave processes is given by [16] (see Refs. [2,15,27] for a general treatment)

$$\Omega_X \approx \xi_f \frac{0.17 \text{ pb}}{\sigma_0} \approx 0.23 \xi_f \frac{1}{k_X} \left(\frac{0.025}{\alpha_X} \frac{m_X}{\text{TeV}} \right)^2, \quad (19)$$

where k_X is an $\mathcal{O}(1)$ constant defined by $\sigma_0 \equiv k_X \pi \alpha_X^2 / m_X^2$, $\alpha_X \equiv g_X^2 / (4\pi)$ is the coupling related to the annihilation process, and $\xi_f \equiv T_f^h / T_f^v$ is the ratio of the hidden to visible sector temperatures when the hidden dark matter freezes out.

For our $U(1)_A \times U(1)_B$ model, dark matter is either composed of Dirac electrons annihilating to A photons through t -channel electrons, or selectrons \tilde{e}_1 annihilating to A photons through t channel selectrons. The annihilation

constants are $k_e = 1$ for the electron and $k_{\tilde{e}_1} = 2$ for the selectron [2,28]. The resulting relic density is

$$\begin{aligned} \Omega_i &\approx 0.23 \xi_f \frac{1}{k_i} \left(\frac{0.025}{\alpha_A} \frac{m_i}{\text{TeV}} \right)^2 \\ &= 0.23 \frac{f_i(\tilde{g}_B, \tilde{y}_e, \tilde{y}_\mu)}{k_i} \left(\frac{\sqrt{\xi_f} M_{3/2}}{126 \text{ TeV}} \right)^2, \end{aligned} \quad (20)$$

where $i = e$ or \tilde{e}_1 , and we have defined the dimensionless quantity

$$f_i(\tilde{g}_B, \tilde{y}_e, \tilde{y}_\mu) \equiv \frac{m_i^2}{M_A^2}, \quad (21)$$

which depends only on the ratio of couplings. The relic density is therefore independent of the overall scale of the couplings, as expected for WIMPlless dark matter. For every point in the parameter space, $\sqrt{\xi_f} M_{3/2}$ is fixed by the relic density. In Fig. 2, $\sqrt{\xi_f} M_{3/2}$ is plotted for the $\tilde{y}_\mu = 5$ and $\tilde{g}_B = 1$ sections of the parameter space.

The gravitino mass in AMSB is bounded by colliders. LEP2 constraints require Wino masses $m_{\tilde{W}} > 92\text{--}103$ GeV, depending on the chargino-neutralino mass difference [29]. Assuming the minimal AMSB relation for the Wino mass, this implies $M_{3/2} \simeq 370 m_{\tilde{W}} \gtrsim 34\text{--}38$ TeV. The LHC also bounds the gravitino mass, but these constraints depend on the spectrum of strongly-interacting superpartners. As an example, in the framework of minimal AMSB [30,31], where a universal scalar mass m_0 is added to solve the tachyonic slepton problem, null results

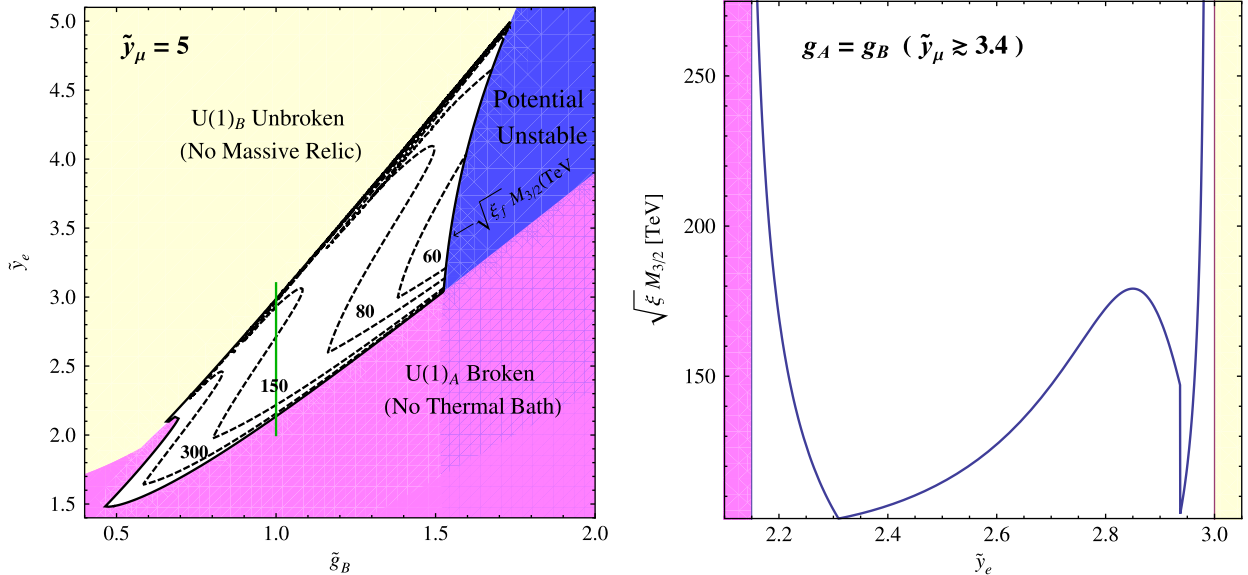


FIG. 2 (color online). *Left*: Contours of constant $\sqrt{\xi_f} M_{3/2}$ as determined by the dark matter relic density in the $(\tilde{g}_B, \tilde{y}_e)$ plane for fixed $\tilde{y}_\mu = 5$. The shaded regions are excluded for the reasons indicated. The green line segment at $\tilde{g}_B = 1$ indicates the domain for the plot in the right panel. *Right*: $\sqrt{\xi_f} M_{3/2}$ as a function of \tilde{y}_e for fixed $\tilde{g}_B = 1$. This curve is independent of \tilde{y}_μ , as long as $\tilde{y}_\mu \gtrsim 3.4$, so that the potential is stable for the entire \tilde{y}_e range. Note the cusp at $\tilde{y}_e \sim 2.31$ and the discontinuity at $\tilde{y}_e \sim 2.94$, which correspond to the dark matter making a transition from one selectron mass eigenstate to another, and from a selectron to an electron, respectively. We have used the same shading as in the left panel to indicate excluded regions.

from the 0-lepton search by ATLAS [32] imply $M_{3/2} \gtrsim 30\text{--}40$ TeV, depending on the value of m_0 [33]. These bounds are also presumably relaxed if R parity is violated, a viable possibility, since the stability of dark matter does not require R -parity conservation in this model.

From a low-energy phenomenological approach, a 40 TeV gravitino would seem most natural. Moreover, cosmological considerations lead us to expect $\xi_f \sim 1$, which would result, for example, from the case where the hidden and visible sectors were in thermal contact at early times. This points toward $\sqrt{\xi_f} M_{3/2} \sim \mathcal{O}(100 \text{ TeV})$. Figure 2 shows that such values are typical in this model, and the desired thermal relic density is generically obtained, as expected for a realization of the WIMPLESS miracle.

V. EFFECTS FROM NEW RELATIVISTIC DEGREES OF FREEDOM

A. g_* and ξ at freeze-out

As was pointed out earlier, our model introduces several massless particles. Their existence may be used for estimating the value of ξ_f in Eq. (20). To see this, define $g_*(T)$ to be the number of relativistic degrees of freedom at temperature T . Assuming entropy conservation, the ratio of temperatures at freeze-out is given by

$$\xi_f = \left[\frac{g_*^h(T_\infty^h)}{g_*^h(T_f^h)} \frac{g_*^v(T_f^v)}{g_*^v(T_\infty^v)} \right]^{(1/3)} \xi_\infty, \quad (22)$$

where ξ_∞ is the temperature ratio of the hidden and visible sectors at very early (and very hot) times, and the superscripts ‘‘h’’ and ‘‘v’’ denote hidden and visible sector quantities, respectively. In full generality, the value of ξ_f depends on the field content at all possible scales in both sectors. However, assuming there are no particles with masses between the temperature at which the two sectors thermally decoupled and the masses of the heaviest particles we have considered, we have $g_*^v(T_\infty^v) = g_*^{\text{MSSM}} = 228.75$. For the hidden sector we have

$$g_*^h(T_\infty^h) = \frac{7}{8}(2 \times 6 + 2 \times 2) + (2 \times 6 + 2 \times 2) = 30. \quad (23)$$

At the time of freeze-out, the massless degrees of freedom in the hidden sector are the photon, the Higgsino \tilde{H}_μ , and the muons, yielding

$$g_*^h(T_f^h) = \frac{7}{8}(4 + 2) + (2) = \frac{29}{4}. \quad (24)$$

Equation (22) then gives

$$\xi_f = 1.25 \left[\frac{g_*^v(T_f^v)}{106.75} \right]^{(1/3)} \xi_\infty, \quad (25)$$

where we have normalized $g_*^v(T_f^v)$ to the total SM degrees of freedom $g_*^{\text{SM}} = 106.75$. Assuming thermal contact at early times ($\xi_\infty = 1$), the value of ξ_f remains close to 1, which makes it easy to reinterpret the contours in Fig. 2 as

curves of constant $M_{3/2}$. Recall that the lower bound from LHC is $M_{3/2} \gtrsim 30\text{--}40$ TeV. Note, however, that Eq. (25) relies on the assumption of a ‘‘high energy desert,’’ as discussed above. Moreover, light dark matter would imply lower $g_*^v(T_f^v)$ values, thereby decreasing ξ_f/ξ_∞ .

B. Bounds from CMB and BBN

The massless particles of the hidden sector contribute to the number of relativistic degrees of freedom at any temperature. Their existence is therefore constrained by the standard theory of BBN and by observations of the CMB. It is customary to measure the number of extra degrees of freedom in units of the effective number of extra neutrinos ΔN_{eff} , as if these were new active neutrino species contributing to the energy density of the Universe. Currently, some of the more stringent bounds on ΔN_{eff} are

$$\Delta N_{\text{eff}} = 0.19 \pm 1.2 \text{ (95\% C.L.) BBN} \quad (26)$$

[34,35],

$$\Delta N_{\text{eff}} = 1.51 \pm 0.75 \text{ (68\% C.L.) CMB (ACT)} \quad (27)$$

[36],

$$\Delta N_{\text{eff}} = 0.81 \pm 0.42 \text{ (68\% C.L.) CMB (SPT)} \quad (28)$$

[37], where the BBN constraint assumes a baryon density that has been fixed to the value determined by the CMB, and both ${}^4\text{He}$ and D data are included, and the CMB constraints combine data from the indicated experiments with WMAP 7-year results [38], distance information from baryon acoustic oscillations, and Hubble constant measurements. The BBN result is fully consistent with the standard model, but with relatively large uncertainty, while the CMB results have smaller uncertainties and show 2σ excesses. In the near future, the uncertainty in the measurement by Planck is expected to drop to ~ 0.3 [39–42], given only ~ 1 year of data. This should improve further as soon as more data is acquired, and a future LSST-like survey may determine ΔN_{eff} with an accuracy within 0.1 [42]. The current status of ΔN_{eff} has generated a great deal of interest; for recent reviews and possible explanations, see, for example, Refs. [43,44].

In the present context, we can express ΔN_{eff} in terms of g_*^h and the temperature:

$$\Delta N_{\text{eff}} \frac{7}{8} 2 T_\nu^4 = g_*^h(T_{\text{CMB}}^h) T_{\text{CMB}}^4, \quad (29)$$

where $T_\nu = (4/11)^{1/3} T_{\text{CMB}}^v$. Assuming entropy conservation, the values of g_* at freeze-out and as measured by the CMB are related through

$$\xi_{\text{CMB}} = \left[\frac{g_*^h(T_f^h)}{g_*^h(T_{\text{CMB}}^h)} \frac{g_*^v(T_{\text{CMB}}^v)}{g_*^v(T_f^v)} \right]^{1/3} \xi_f. \quad (30)$$

Using this relation, we get

$$\begin{aligned}\Delta N_{\text{eff}} &= \frac{4}{7} \left(\frac{11}{4}\right)^{4/3} g_*^{\text{h}}(T_{\text{CMB}}^{\text{h}}) \xi_{\text{CMB}}^4 \\ &= \frac{4}{7} \left(\frac{11}{4}\right)^{4/3} g_*^{\text{h}}(T_{\text{CMB}}^{\text{h}}) \left[\frac{g_*^{\text{h}}(T_f^{\text{h}})}{g_*^{\text{h}}(T_{\text{CMB}}^{\text{h}})} \frac{g_*^{\text{v}}(T_{\text{CMB}}^{\text{v}})}{g_*^{\text{v}}(T_f^{\text{v}})} \right]^{4/3} \xi_f^4.\end{aligned}\quad (31)$$

At the time of CMB decoupling we have $g_*^{\text{v}}(T_{\text{CMB}}^{\text{v}}) = 2$ and $g_*^{\text{h}}(T_f^{\text{h}}) = g_*^{\text{h}}(T_{\text{CMB}}^{\text{h}}) = 29/4$. This implies

$$\Delta N_{\text{eff}} = \left(\frac{\xi_f}{1.88}\right)^4 \left[\frac{106.75}{g_*^{\text{v}}(T_f^{\text{v}})}\right]^{4/3}.\quad (32)$$

We may use now Eq. (25) to express the effective number of extra neutrinos in terms of ξ_{∞} . Under the assumption of a high energy desert we obtain

$$\Delta N_{\text{eff}} = 0.19 \xi_{\infty}^4.\quad (33)$$

Moreover, note that Eq. (33) is independent of $g_*^{\text{v}}(T_f^{\text{v}})$, giving a sharp prediction once the two assumptions of a high energy desert and thermal contact at early times ($\xi_{\infty} = 1$) are made. Such a prediction is interesting, especially given the bright prospects for improved measurements of ΔN_{eff} in the near future.

Alternatively, given $M_{3/2}$, we can obtain ξ_f as a function of the parameter space, as determined by the relic density condition. This implies, through Eq. (32), that ΔN_{eff} is determined as well. In Fig. 3, ΔN_{eff} is plotted for

the sections of parameter space defined by $\tilde{y}_{\mu} = 5$ and $\tilde{g}_B = 1$. Note, however, that ΔN_{eff} is highly sensitive to $M_{3/2}$: for a fixed relic density, $\Delta N_{\text{eff}} \propto M_{3/2}^{-8}$.

VI. SELF-INTERACTIONS

So far, all the observables we have discussed depend only on ratios of couplings. This scaling is a key feature of WIMPLESS dark matter. However, some observations constrain absolute coupling values, rather than just ratios.

An example is constraints from structure formation. The dark matter described in this work has a hidden charge, and is therefore subject to constraints on self-interactions through a long-range force. In Refs. [28,45], bounds on dark matter mass and coupling were derived from the observation of elliptical halos. Following earlier work [46], the authors used measurements that established the ellipticity of the galaxy NGC 720 [47,48]. Strong enough self-interactions would tend to turn elliptic halos into spheres over the course of a cosmological time scale, leading to the bound

$$\left(\frac{m_X}{22 \text{ TeV}}\right)^3 \gtrsim \alpha_X^2.\quad (34)$$

Using $\alpha_A = \pi M_{\tilde{A}}/M_{3/2}$ and Eq. (21), we obtain the lower bound

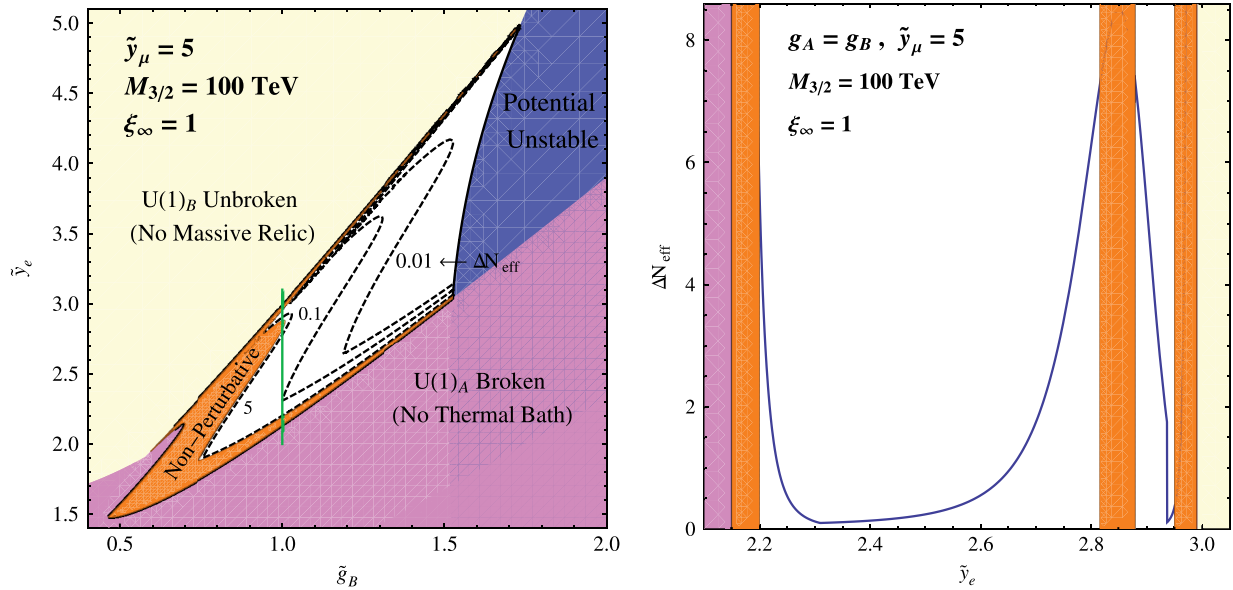


FIG. 3 (color online). *Left*: Contours of constant ΔN_{eff} in the $(\tilde{g}_B, \tilde{y}_e)$ plane for fixed $\tilde{y}_{\mu} = 5$, $M_{3/2} = 100 \text{ TeV}$, and $\xi_{\infty} = 1$. The shaded regions are excluded for the reasons indicated. The orange region, labeled “Non-Perturbative,” is excluded by considerations of self-interactions and perturbativity, as explained in Sec. VI. The green line segment at $g_A = g_B$ indicates the domain taken for the plot in the right panel. *Right*: ΔN_{eff} as a function of \tilde{y}_e for the same parameters as in the left panel and $\tilde{g}_B = 1$. This curve is independent of \tilde{y}_{μ} , as long as $\tilde{y}_{\mu} \gtrsim 3.4$, so that the potential is stable for the entire \tilde{y}_e range. We have used the same shading as in the left panel to indicate excluded regions.

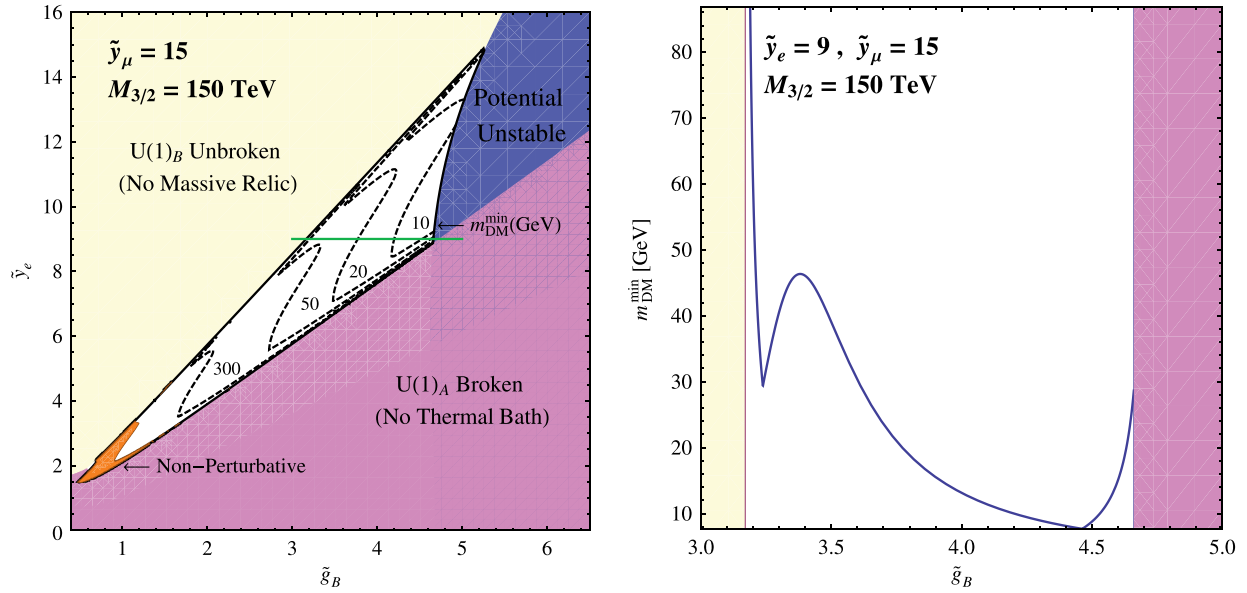


FIG. 4 (color online). *Left*: Contours of constant $m_{\text{DM}}^{\text{min}}$ in the $(\tilde{g}_B, \tilde{y}_e)$ plane for fixed $\tilde{y}_\mu = 15$ and $M_{3/2} = 150$ TeV. The shaded regions are excluded for the reasons indicated. The green line segment at $\tilde{y}_e = 9$ indicates the domain taken for the plot in the right panel. *Right*: The minimum dark matter mass $m_{\text{DM}}^{\text{min}}$ as a function of \tilde{g}_B for the same parameters as in the left panel and $\tilde{y}_e = 9$. This curve is independent of \tilde{y}_μ , as long as $\tilde{y}_\mu \gtrsim 3.4$, so that the potential is stable for the entire \tilde{y}_e range. We have used the same shading as in the left panel to indicate excluded regions.

$$m_i \gtrsim \frac{10 \text{ TeV}}{f_i(\tilde{g}_B, \tilde{y}_e, \tilde{y}_\mu)} \left(\frac{100 \text{ TeV}}{M_{3/2}} \right)^2 \equiv m_{\text{DM}}^{\text{min}}, \quad (35)$$

where i denotes either e or \bar{e}_1 , depending on the identity of the dark matter particle at the particular point of parameter space.

This lower bound on the dark matter mass also sets a lower bound on the mass of the heaviest particle in the spectrum at each point in the parameter space. However, our description above relies on a perturbative expansion that is valid as long as all particle masses (and, in particular, the heaviest particle mass) are below $M_{3/2}$ [16]. As a result, certain regions in the parameter space are excluded for a given $M_{3/2}$. Figure 4 shows contours of constant $m_{\text{DM}}^{\text{min}}$ according to Eq. (35). Regions that are forbidden by perturbativity (or breakdown of the effective field theory) are shown as well. As can be seen in the figure, dark matter can be as light as a few GeV for reasonable values of $M_{3/2}$ and \tilde{y}_μ . Smaller dark matter masses are also possible if one tunes parameters to more extreme values. Values of dark matter mass ~ 10 GeV are of special interest, given reported direct detection signals of dark matter with such masses. Of course, a complete explanation of such signals requires coupling the hidden sector to the visible sector, which we have not done in this paper.

VII. SUMMARY AND DISCUSSION

In this work, we have presented a model for WIMPLESS dark matter from a hidden sector with AMSB. The novel feature of this work is that dark matter in a hidden sector

naturally has the correct relic density, in the sense that it is determined purely by the soft SUSY-breaking scale, without the introduction and tuning of other dimensionful parameters. The correct relic density therefore emerges naturally, in the same sense as for WIMPs, but the dark matter may have very different masses and interaction strengths.

Our new model has a $U(1) \times U(1)$ gauge symmetry. One $U(1)$ provides massless hidden photons for the thermal bath, and the second $U(1)$ is broken spontaneously by a Higgs field. The matter field content includes a family of three chiral superfields, and its mirror family, with all the charges inverted. The mirror family is required for the cancellation of chiral anomalies, but we prevent renormalizable supersymmetric interfamily couplings by imposing a Z_3 symmetry, such that all the fields have the same triality. Symmetries therefore forbid the introduction of new mass scales. The symmetries also guarantee the stability of a massive dark matter candidate. R -parity conservation is not required, and so the visible sector may appear at colliders through R -parity violating signals. We note, however, that since the Z_3 symmetry is spontaneously broken, the model suffers from domain wall problems, similar to those of the next-to-minimal supersymmetric standard model. We assume that these may be overcome through similar mechanisms (for discussions, see, for example, Refs. [49–51]), but a detailed investigation is beyond the scope of this work.

The dark matter spectrum depends on two gauge and two Yukawa couplings, while annihilation depends exclusively on the gauge coupling of the unbroken $U(1)$.

However, the relic density depends only on ratios of couplings, and not on their overall scale. For nonhierarchical couplings, the correct relic density is obtained, irrespective of the dark matter's mass or interaction strength, thereby realizing the WIMPless miracle.

The model includes new relativistic degrees of freedom contributing to the energy density of the Universe at freeze-out and at late times. In a significant region of the parameter space, nonzero values of ΔN_{eff} are predicted. This observable is now being probed by the Planck observatory. This model also predicts dark matter that self-interacts through long-range interactions. Such self-interactions are constrained by elliptical halo shapes. However, a positive signal of self-interacting dark matter would fix the ratio $m_{\text{DM}}^3/\alpha_{\text{DM}}^2$, and therefore determine the dark matter's actual mass. In the absence of such observation, the self-interaction implies a lower bound on the dark matter mass. Regions in the parameter space where this bound is low (for example, below 10 GeV for $\tilde{y}_\mu = 15$ and $M_{3/2} = 150$ TeV) are allowed.

It would be interesting to relieve the constraints imposed by galactic halo shapes by giving the hidden photon a small mass. Such a massive photon would be overabundant, unless it is allowed to decay, for example, via kinetic mixing with the visible photon. This scenario is different compared to the one we have discussed so far, in both its early Universe cosmology and dark matter phenomenology. In this case, the model typically predicts a smaller contribution to ΔN_{eff} , and the two sectors are thermalized,

implying $\xi_f = 1$. Moreover, charged particles in the visible sector become millicharged under the hidden $U(1)$, while dark matter remains electrically neutral. Phenomenological implications of such dark forces have been studied in a number of papers; see, e.g., Refs. [52,53]. Since the dark matter in this case may be light, it could in principle explain the recent signals from CoGeNT, DAMA, or CRESST. In addition, there may also be other phenomenological implications for indirect detection, collider physics, and low-energy laboratory experiments [54].

Last, the embedding of dark matter in AMSB might raise the question of implications from recent LHC data, and, in particular, constraints on AMSB from null results of SUSY searches [33] and hints of a possible SM-like Higgs boson at 124–126 GeV [55,56]. These results generally disfavor light superpartners. We note, however, that the hidden dark matter properties described here are largely insensitive to the details of the visible sector, and as long as AMSB models with $M_{3/2} \sim 100$ TeV are viable, the essential motivations and features of these models remain.

ACKNOWLEDGMENTS

We thank M. Kaplinghat, Y. Shirman, and Y. Shadmi for helpful conversations. The work of J. L. F. was supported in part by the NSF under Grant No. PHY-0970173. The work of V. R. was supported in part by the DOE under Grant No. DE-FG02-04ER-41298.

-
- [1] J. L. Feng and J. Kumar, *Phys. Rev. Lett.* **101**, 231301 (2008).
 - [2] J. L. Feng, H. Tu, and H.-B. Yu, *J. Cosmol. Astropart. Phys.* 10(2008) 043.
 - [3] J. L. Feng, J. Kumar, and L. E. Strigari, *Phys. Lett. B* **670**, 37 (2008).
 - [4] J. L. Feng, J. Kumar, J. Learned, and L. E. Strigari, *J. Cosmol. Astropart. Phys.* 01 (2009) 032.
 - [5] J. Kumar, J. G. Learned, and S. Smith, *Phys. Rev. D* **80**, 113002 (2009).
 - [6] V. Barger, J. Kumar, D. Marfatia, and E. M. Sessolo, *Phys. Rev. D* **81**, 115010 (2010).
 - [7] G. Zhu, *Phys. Rev. D* **83**, 076011 (2011).
 - [8] D. McKeen, *Phys. Rev. D* **79**, 114001 (2009).
 - [9] G. K. Yeghiyan, *Phys. Rev. D* **80**, 115019 (2009).
 - [10] D. McKeen, *Ann. Phys. (N.Y.)* **326**, 1501 (2011).
 - [11] A. Badin and A. A. Petrov, *Phys. Rev. D* **82**, 034005 (2010).
 - [12] J. Alwall, J. L. Feng, J. Kumar, and S. Su, *Phys. Rev. D* **81**, 114027 (2010).
 - [13] J. Goodman *et al.*, *Phys. Rev. D* **82**, 116010 (2010).
 - [14] J. Alwall, J. L. Feng, J. Kumar, and S. Su, *Phys. Rev. D* **84**, 074010 (2011).
 - [15] J. L. Feng and Y. Shadmi, *Phys. Rev. D* **83**, 095011 (2011).
 - [16] J. L. Feng, V. Rentala, and Z. Surujon, *Phys. Rev. D* **84**, 095033 (2011).
 - [17] L. Randall and R. Sundrum, *Nucl. Phys.* **B557**, 79 (1999).
 - [18] G. F. Giudice, M. A. Luty, H. Murayama, and R. Rattazzi, *J. High Energy Phys.* 12 (1998) 027.
 - [19] G. D'Ambrosio, G. Giudice, G. Isidori, and A. Strumia, *Nucl. Phys.* **B645**, 155 (2002).
 - [20] A. Buras, P. Gambino, M. Gorbahn, S. Jager, and L. Silvestrini, *Phys. Lett. B* **500**, 161 (2001).
 - [21] L. Hall and L. Randall, *Phys. Rev. Lett.* **65**, 2939 (1990).
 - [22] R. Chivukula and H. Georgi, *Phys. Lett. B* **188**, 99 (1987).
 - [23] A. Pomarol and R. Rattazzi, *J. High Energy Phys.* 05 (1999) 013.
 - [24] Z. Chacko, M. A. Luty, I. Maksymyk, and E. Ponton, *J. High Energy Phys.* 04 (2000) 001.
 - [25] E. Katz, Y. Shadmi, and Y. Shirman, *J. High Energy Phys.* 08 (1999) 015.
 - [26] B. C. Allanach and A. Dedes, *J. High Energy Phys.* 06 (2000) 017.
 - [27] S. Das and K. Sigurdson, [arXiv:1012.4458](https://arxiv.org/abs/1012.4458).
 - [28] J. L. Feng, M. Kaplinghat, H. Tu, and H.-B. Yu, *J. Cosmol. Astropart. Phys.* 07 (2009) 004.

- [29] J. L. Feng, J.-F. Grivaz, and J. Nachtman, *Rev. Mod. Phys.* **82**, 699 (2010).
- [30] T. Gherghetta, G. F. Giudice, and J. D. Wells, *Nucl. Phys.* **B559**, 27 (1999).
- [31] J. L. Feng and T. Moroi, *Phys. Rev. D* **61**, 095004 (2000).
- [32] G. Aad *et al.* (ATLAS Collaboration), *Phys. Lett. B* **701**, 186 (2011).
- [33] B. Allanach, T. Khoo, and K. Sakurai, *J. High Energy Phys.* **11** (2011) 132.
- [34] R. H. Cyburt, B. D. Fields, K. A. Olive, and E. Skillman, *Astropart. Phys.* **23**, 313 (2005).
- [35] B. Fields and S. Sarkar, *J. Phys. G* **33**, 1 (2006).
- [36] J. Dunkley *et al.*, *Astrophys. J.* **739**, 52 (2011).
- [37] R. Keisler *et al.*, *Astrophys. J.* **743**, 28 (2011).
- [38] E. Komatsu *et al.* (WMAP Collaboration), *Astrophys. J. Suppl. Ser.* **192**, 18 (2011).
- [39] J. Hamann, J. Lesgourgues, and G. Mangano, *J. Cosmol. Astropart. Phys.* **03** (2008) 004.
- [40] K. Ichikawa, T. Sekiguchi, and T. Takahashi, *Phys. Rev. D* **78**, 083526 (2008).
- [41] L. Colombo, E. Pierpaoli, and J. Pritchard, *Mon. Not. R. Astron. Soc.* **398**, 1621 (2009).
- [42] S. Joudaki and M. Kaplinghat, [arXiv:1106.0299](https://arxiv.org/abs/1106.0299).
- [43] J. Hamann, S. Hannestad, G. G. Raffelt, and Y. Y. Y. Wong, *J. Cosmol. Astropart. Phys.* **09** (2011) 034.
- [44] J. L. Menestrina and R. J. Scherrer, *Phys. Rev. D* **85**, 047301 (2012).
- [45] L. Ackerman, M. R. Buckley, S. M. Carroll, and M. Kamionkowski, *Phys. Rev. D* **79**, 023519 (2009).
- [46] J. Miralda-Escudé, *Astrophys. J.* **564**, 60 (2002).
- [47] D. A. Buote, T. E. Jeltema, C. R. Canizares, and G. P. Garmire, *Astrophys. J.* **577**, 183 (2002).
- [48] P. J. Humphrey *et al.*, *Astrophys. J.* **646**, 899 (2006).
- [49] J. Preskill, S. P. Trivedi, F. Wilczek, and M. B. Wise, *Nucl. Phys.* **B363**, 207 (1991).
- [50] S. Abel, S. Sarkar, and P. White, *Nucl. Phys.* **B454**, 663 (1995).
- [51] U. Ellwanger, C. Hugonie, and A. M. Teixeira, *Phys. Rep.* **496**, 1 (2010).
- [52] R. Essig, P. Schuster, and N. Toro, *Phys. Rev. D* **80**, 015003 (2009).
- [53] G. Amelino-Camelia *et al.*, *Eur. Phys. J. C* **68**, 619 (2010).
- [54] T. Lin, H.-B. Yu, and K. M. Zurek, [arXiv:1111.0293](https://arxiv.org/abs/1111.0293).
- [55] F. Giannotti (ATLAS Collaboration), CERN Public Seminar, December 13, 2011, <https://indico.cern.ch/conferenceDisplay.py?confId=164890>.
- [56] G. Tonelli (CMS Collaboration), CERN Public Seminar, December 13, 2011, <https://indico.cern.ch/conferenceDisplay.py?confId=164890>.